RESEARCH ARTICLE

CLIMATE VARIABILITY

Multidecadal climate oscillations during the past millennium driven by volcanic forcing

Michael E. Mann[1]*, Byron A. Steinman[2], Daniel J. Brouillette[1], Sonya K. Miller[1]

Past research argues for an internal multidecadal (40- to 60-year) oscillation distinct from climate noise. Recent studies have claimed that this so-termed Atlantic Multidecadal Oscillation is instead a manifestation of competing time-varying effects of anthropogenic greenhouse gases and sulfate aerosols. That conclusion is bolstered by the absence of robust multidecadal climate oscillations in control simulations of current-generation models. Paleoclimate data, however, do demonstrate multidecadal oscillatory behavior during the preindustrial era. By comparing control and forced "Last Millennium" simulations, we show that these apparent multidecadal oscillations are an artifact of pulses of volcanic activity during the preindustrial era that project markedly onto the multidecadal (50- to 70-year) frequency band. We conclude that there is no compelling evidence for internal multidecadal oscillations in the climate system.

An analysis of state-of-the-art climate model simulations spanning the past millennium provides no evidence for an internally generated, multidecadal oscillatory Atlantic Multidecadal Oscillation (AMO) signal in the climate system and instead suggests the presence of a 50- to 70-year "AMO-like" signal driven by episodes of high-amplitude explosive volcanism with multidecadal pacing.

Modes of internal climate system variability, such as the El Niño–Southern Oscillation (ENSO), lead to interannual oscillatory behavior, i.e., coherent large-scale variability with a well-defined time scale, distinct from simple "red noise." Researchers, however, continue to debate the existence of longer-term oscillatory internal modes of climate variability. Past research analyzing observations, paleoclimate proxies, and model simulations has argued for distinct interdecadal (*1*–*11*) and multidecadal (*8*, *9*, *12*–*15*) climate oscillations, but more recent work (*16*–*27*) has challenged these findings.

Evidence for a 50- to 70-year North Atlantic–centered oscillation originated in observational studies by Folland and colleagues during the 1980s (*12*, *13*). In the 1990s, Mann and Park (*8*, *9*) and Tourre *et al*. (*14*) applied a multivariate signal detection approach (the multitaper method singular value decomposition or "MTM-SVD" method) to global surface temperature data, to separate distinct long-term surface temperature signals, whereas Schlesinger and Ramankutty (*15*) provided evidence for a residual multidecadal signal using a model to estimate and remove the forced trend from observations. These analyses collectively argued for a multidecadal (50- to 70-year) time-scale signal centered in the North Atlantic, but with hemispheric-scale impacts, which was subsequently termed the Atlantic Multidecadal Oscillation (AMO) (*28*).

The confident identification of a signal has been hampered by the short instrumental climate record and confounding influences of forced long-term climate trends. Though numerous studies have attributed the AMO to internal oscillatory behavior tied to the Atlantic Meridional Overturning Circulation (AMOC) (*29*–*35*), others have dismissed the AMO as the response of North Atlantic surface temperatures to stochastic atmospheric forcing (*17*–*19*) or external radiative forcing (*20*–*24*). Yet others maintain that an internal AMO signal may exist but has been misidentified in studies that do not properly distinguish forced from internal variability (*16*, *25*–*27*).

Spectral analyses of paleoclimate proxy data (*36*, *37*) do show evidence for multidecadal AMO-like oscillations in past centuries. Using the MTM-SVD approach, Mann *et al*. (*36*) found evidence for a statistically significant 50- to 70-year spectral peak in a set of 27 proxy records dating back to 1400 CE. Other recent studies, however, have analyzed proxy-based reconstructions of climate indices (*38*–*42*), yielding conflicting results.

Cook *et al*. (*39*) used tree rings from regions bordering the North Atlantic to reconstruct a winter North Atlantic Oscillation (NAO) index back to 1400 CE and argued that multidecadal oscillations were limited to the modern period, with no evidence prior to 1900 CE. By contrast, D'Arrigo *et al*. (*38*) produced a warm-season Arctic Oscillation (AO) index with North American and Eurasian tree rings and found a multidecadal spectral peak prior to the 20th century. Gray *et al*. (*42*) and Wang *et al*. (*43*) reconstructed a North Atlantic sea-surface temperature (SST)–based AMO index from tree rings back to 1567 CE and 800 CE, respectively. Each found evidence for persistent 50- to 70-year oscillations prior to the 20th century.

Although these AMO reconstructions appear similar during the modern period, they diverge in past centuries (*44*). An important caveat applies to such reconstructions: They require calibration of proxy data against a single index during the modern period, but the governing mechanisms may be different during the modern period and the past. Such problems can be partly avoided using climate-field reconstruction methods that employ multiple independent patterns of variability (*45*).

This caveat holds in the present case. Anthropogenic greenhouse gas and sulfate aerosols affecting North Atlantic temperatures compete during the 20th century (*16*, *25*–*27*) but are weak or absent before this time. The impact of this nonstationarity on calibration procedures may explain the observed divergence in these various AMO-related indices.

Mann *et al*. (*45*) used a global multiproxy dataset to reconstruct surface temperatures over the past millennium. They derived an AMO index averaging over the North Atlantic; however, use of a decreasing number of patterns back in time limits insights into multidecadal variability at regional scales. Fischer and Mieding (*41*) inferred long-term North Atlantic climate variability from Greenland ice cores, but it is difficult to extrapolate North Atlantic–wide climate trends from a single region like Greenland. Singh *et al*. (*40*) used a data-assimilation approach, combining model physics and paleoclimate data by assimilating proxies into two Fifth Coupled Model Intercomparison Project (CMIP5) "Last Millennium" model simulations. Their AMO indices, estimated from reconstructed North Atlantic surface-temperature fields, show no multidecadal spectral peaks. A caveat with data-assimilation approaches is that model states (e.g., atmospheric teleconnection patterns) are typically biased relative to the real world, leading to loss of variance and fidelity in the resulting reconstruction (*46*, *47*).

In summary, there is no well-defined, agreed-upon preinstrumental AMO time series. Consequently, there is no consensus on the relative role of internal variability and external forcing in multidecadal AMO-like variability in past centuries (*46*, *47*). We can nonetheless obtain key insights within the synthetic world of model simulations, where such complications do not apply.

Control coupled ocean-atmosphere model simulations provide an important laboratory for understanding the origins of multidecadal variability because forcing remains constant and oscillatory signals can be attributed to

[1]Department of Meteorology and Atmospheric Science, The Pennsylvania State University, 514 Walker Building, University Park, PA 16802-5013, USA. [2]Department of Earth and Environmental Sciences and Large Lakes Observatory, University of Minnesota Duluth, 2205 East 5th Street, Duluth, MN 55812, USA.
*Corresponding author. Email: mann@psu.edu

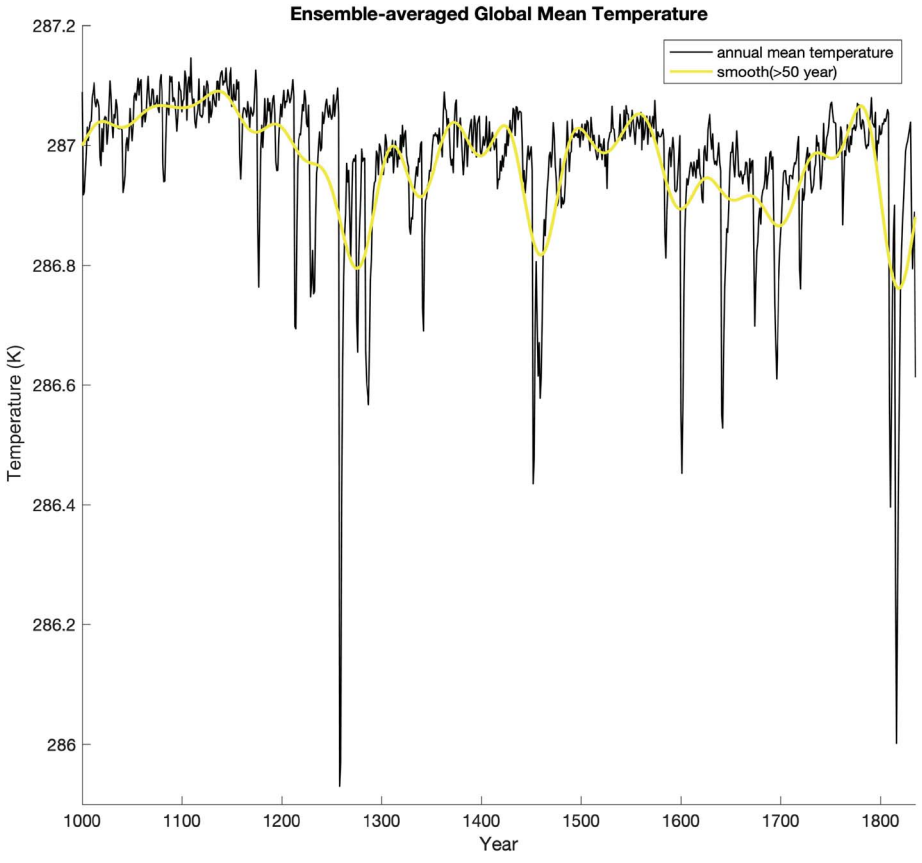

Fig. 1. Ensemble-averaged global mean temperature for CMIP5 Last Millennium experiments (representing the average over *M* = 16 simulations during the 1000–1835 CE overlap of all simulations). Shown are both the raw annual averages (black) and a smoothed [50-year lowpass using the method of Mann (*60*)] version (yellow) of the series, emphasizing the multidecadal and longer-term variability.

internal variability alone. If such signals exist, they should be associated with coherent large-scale patterns of variability with a well-defined time scale that is statistically significant relative to a simple red noise null hypothesis. However, because a prospective signal may largely redistribute heat over Earth's surface (rather than change the global surface heat budget), the signal projection onto hemispheric or global mean temperature may be weak or nonexistent. Any signal detection approach should thus be applied to the full surface temperature field rather than regionally or globally averaged temperature.

The MTM-SVD method of Mann and Park (*8*–*10*), which identifies narrowband spatiotemporal oscillatory signals in multivariate datasets, is well suited to this task. Using the MTM-SVD approach, Delworth and Mann (*48*) provided evidence for a distinct narrowband (40- to 60-year) multidecadal oscillation in a long (1000-year) control simulation of the Geophysical Fluid Dynamics Laboratory (GFDL) coupled model, whereas Knight *et al.* (*49*) found an AMO signal in a 1400-year control simulation of the Hadley Centre (HadCM3) coupled model. In both cases, the signal displayed peak variations of ~0.5°C in the high-latitude North Atlantic but more modest amplitude ~0.1°C variations in tropical Atlantic and hemispheric mean temperature.

Mann *et al.* (*50*) recently used MTM-SVD to analyze global temperature fields from the suite of CMIP5 control simulations for low-frequency oscillatory climate signals. They found no consistent evidence across the ensemble for narrowband signals in the decadal and interdecadal range (contrasting with clear evidence for interannual ENSO signals). Using the CMIP5 historical simulations, they furthermore demonstrated that an AMO-like signal in the modern era is an artifact of competing, time-varying influences from steadily increasing greenhouse gases and the post-1970 ramp-down in sulfate aerosols.

Collectively, these observations are enigmatic. They fail to explain why multidecadal AMO-like oscillations are observed in paleoclimate proxy data prior to the industrial era. One possible reconciliation is that AMO-like oscillations in past centuries might too be forced but by natural changes in solar irradiance and explosive volcanic activity.

Here, we analyze the CMIP5 multimodel "Last Millennium" simulation ensemble, in which models were driven by estimated natural forcing (*51*), for evidence of narrowband AMO-like oscillatory signals using the MTM-SVD method. Using the ensemble mean, wherein internal variability components from individual ensemble members cancel (*26*, *27*, *52*), we also estimate the forced-only temperature response in the model ensemble. We compare against a previous MTM-SVD analysis of CMIP5 control simulations by Mann *et al.* (*50*), where there is no forced variability. Collectively these analyses allow us to assess evidence—in the context of current-generation models—for persistent multidecadal AMO-like oscillations over the past millennium and to determine whether they are externally forced or internally generated.

Results

The CMIP5 Last Millennium multimodel experiments provide a pseudo-ensemble of $N = 16$ simulations (see supplementary materials) driven with estimated natural forcing (volcanic and solar, with minor additional contributions from astronomical, greenhouse gases, and land-use change) over the preindustrial period (the interval 1000 to 1835 CE is common to all simulations). We estimate the forced-only component of temperature variation by averaging over the ensemble, based on the principle that independent noise realizations cancel in an ensemble mean (*16*, *25*–*27*). The multidecadal variation in ensemble-averaged global mean temperature (Fig. 1) (highlighted; ~0.3°C typical peak-to-peak amplitude), notably, is dominated by the cooling response to major volcanic forcing episodes.

We used MTM-SVD to assess evidence for narrowband multidecadal oscillatory signals in the individual CMIP5 surface temperature fields. MTM-SVD performs a spatiotemporal decomposition of data locally in the frequency domain, determining whether any large-scale pattern within a narrow frequency band describes a larger fraction of variance than would be expected for colored noise (including the standard "red noise" null hypothesis invoked in climate studies). The fractional variance, as a function of frequency [the "local fractional variance" (LFV) spectrum], yields a detection variable, with significance levels estimated by Monte Carlo simulations (see materials and methods).

Comparing the LFV spectra for the CMIP5 control ensemble from Mann *et al.* (*50*) (Fig. 2A) with those for the Last Millennium ensemble (Fig. 2B) reveals pronounced differences. In the former case, as noted earlier, there is no ensemble-wide evidence for a multidecadal spectral peak, with no structure evident in the ensemble mean LFV spectrum over the decadal and multidecadal frequency range. In the latter case, however, we see substantial structure, with peaks common to numerous members of

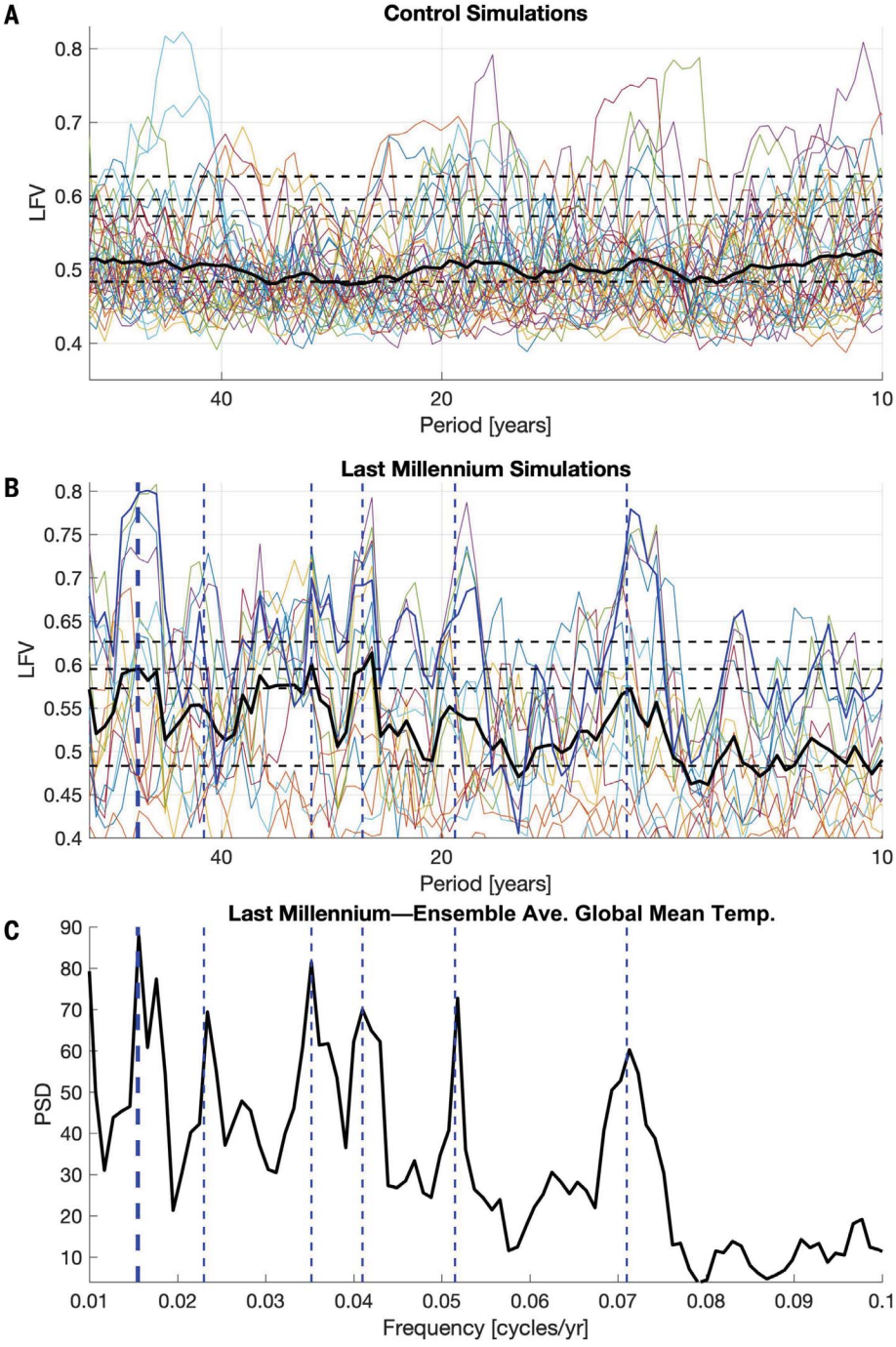

Fig. 2. Spectra for CMIP5 surface temperature data. (**A**) MTM-SVD local fraction variance (LFV) spectrum for CMIP5 control simulations. Individual colored curves depict results for all N = 44 simulations, whereas the ensemble mean is shown by the thick black curve. Lower (f = 0.01 cycle per year) and upper (f = 0.1 cycle per year) bounds on frequencies shown correspond to the edge of the secular band and decadal band, respectively. Horizontal dashed lines correspond to median (p = 0.5) and p = 0.1, 0.05, and 0.01 significance levels relative to colored noise null hypothesis. (**B**) Same as (A) but for the N = 16 CMIP5 Last Millennium simulations (the more prominent blue curve denotes the GISS-E2-R simulation examined in Fig. 3). (**C**) MTM power spectral density of the ensemble-averaged global mean temperature series shown in Fig. 1 over the same frequency range as above, as calculated using the multitaper spectral analysis routine described in Mann and Lees (*52*). The vertical blue dashed lines show the peaks that are common between (B) and (C) (thick dashed line denotes the multidecadal 50- to 70-year period signal of interest).

the ensemble and statistically significant at the $p < 0.05$ level in the ensemble mean in the ~20- to 30-year interdecadal range (centered at frequency f = 0.04 cycle per year) and ~50- to 70-year multidecadal range (centered at f = 0.016 cycle per year). The latter breaches the p = 0.1 significance level for 12 of 16 ensemble members (11 at the p = 0.01 level) and for 6 of 8 of the distinct models (see supplementary materials for further details).

The power spectrum (Fig. 2C) of the CMIP5 ensemble-averaged global temperature series of Fig. 1 exhibits spectral peaks at the same frequencies (e.g., f ~ 0.04 and f ~ 0.016) as the LFV spectra for the full temperature fields (Fig. 2B). Because the structure in the ensemble-averaged global mean series reflects forced variability alone, the origin of the spectral peaks in the LFV spectra can be presumed to be the same—i.e., driven by long-term changes in radiative forcing, primarily the volcanic forcing, which happens to contain a pronounced multidecadal periodicity (*53*). Although solar-only and volcanic-only simulations are not part of the CMIP5 Last Millennium experiment protocol, simulations with an energy-balance model (EBM) driven by the CMIP5 forcing series (supplementary materials) show that the multidecadal spectral peak arises from volcanic forcing alone. Indeed, of the four simulations lacking a multidecadal LFV peak, volcanic forcing turns out to be absent in two models.

To examine the detailed characteristics of the signal, we focus on the simulation (one of the nine GISS-E2-R simulations) that displays the largest LFV spectral peak, but similar results apply to other simulations (see supplementary materials). The signal is characterized by its spatial pattern of explained variance (Fig. 3A), its time-domain projection using a reference gridbox in the tropical Atlantic (Fig. 3B), and the characteristic spatio-temporal evolution over a typical (~60-year) "oscillation" (Fig. 4).

The spatial pattern of variance (Fig. 3A) shows the highest amplitude in the tropics, consistent with the established pattern of response to tropical volcanic forcing. There is also an indication of coupling to extra-tropical atmospheric and oceanic dynamics. Especially notable is the prominent signature in the North Atlantic, where an enhanced signal is seen in the vicinity of the Gulf Stream and North Atlantic drift, and well into the extratropical and subpolar North Atlantic.

In examining the temporal projection of the signal (Fig. 3B), the apparent multidecadal oscillation, as originally hinted at in Fig. 1, is seen to be associated with a response to well-spaced pulses of tropical volcanic activity, with major troughs almost exclusively corresponding to prominent volcanic forcing episodes.

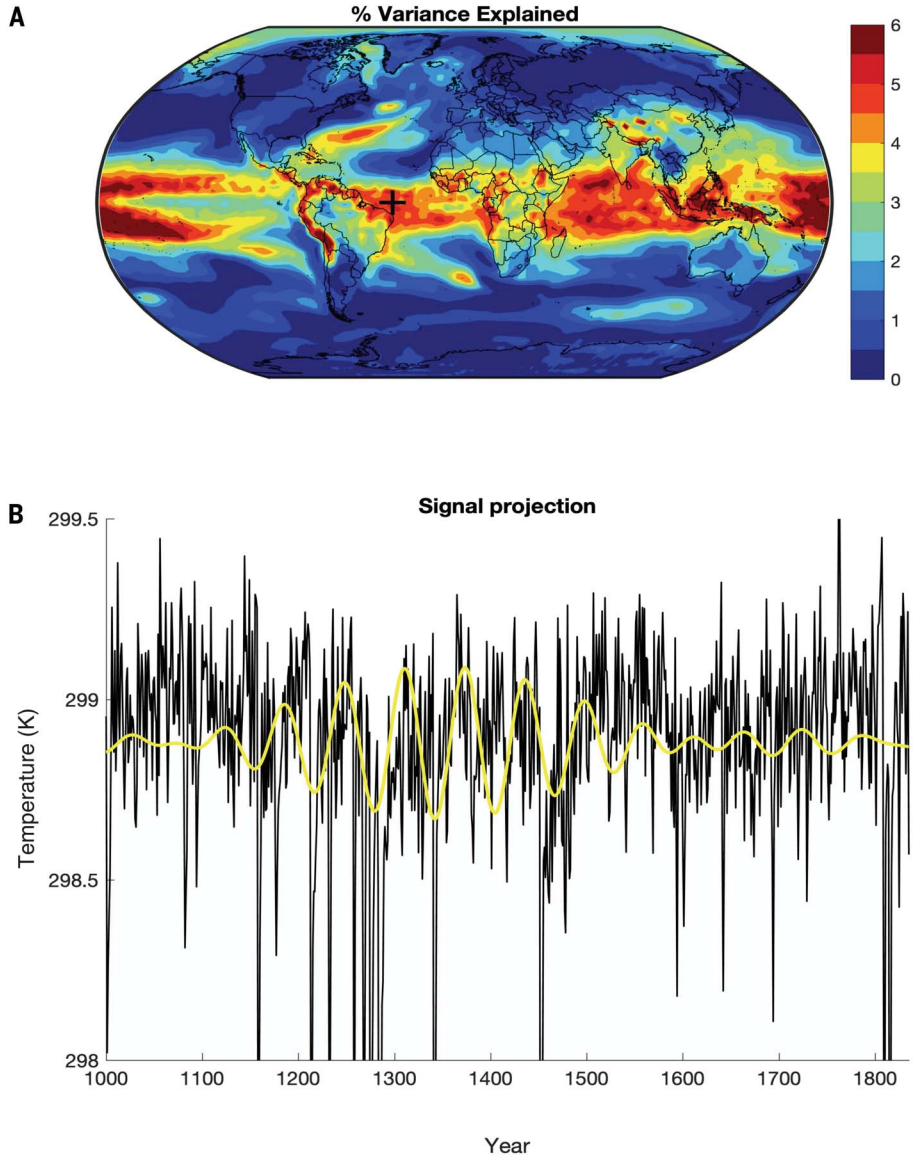

Fig. 3. Spatial and temporal characteristics of multidecadal "signal" (centered at f = 0.016 cycle per year, ~63-year period) for CMIP5 GISS E2-R Last Millennium simulation. (**A**) Spatial pattern of percentage resolved variance associated with signal and (**B**) reconstructed time-domain signal for representative equatorial eastern Atlantic grid box (grid box centered on longitude 35°W and latitude 0°; location denoted by the large black "+" in (A)].

The connection with volcanic forcing is also observed in the spatiotemporal evolution of the signal (Fig. 4). We adopt the convention that the t = 0 (zero phase) pattern corresponds to the peak tropical (and global mean) cooling, i.e., the main expected direct response to volcanic forcing. The pattern also shows evidence of extratropical linkages, including a dynamical AO or NAO-like response in the Northern Hemisphere (*54*) and a warming off Antarctica, consistent with a dynamical coupling with the Southern Annular Mode (*55*–*57*).

The signal evolution over the subsequent quarter cycle (from t = 0 to t = 16-year lag, i.e., 90° phase) suggests a possible additional role for delayed ocean-dynamical responses. Of particular interest is the horseshoe pattern of warming and cooling that develops in extratropical North Atlantic SSTs, reminiscent of the pattern of AMO-like internal variability noted in some simulations (*48*, *49*).

Discussion

Our analysis reveals a robust multidecadal, narrowband (50- to 70-year) oscillatory "AMO-like" signal in simulations of the past millennium; the oscillation is driven by episodes of high-amplitude explosive volcanism that happen, in past centuries, to display a multidecadal pacing. We find no evidence for an internally generated 50- to 70-year multidecadal oscillatory signal despite continued claims that proxy data reveal such a signal (*58*).

We reconcile some apparent contradictions in past work. Our analysis, for example, supports previous studies arguing for a multidecadal (50- to 70-year) spectral peak in AMO-related proxy records and index reconstructions (*36*–*38*, *42*, *43*) and supports past studies that attribute this signal at least partly to natural radiative forcing (*43*, *44*). Where our findings differ from these latter studies, however, is in the degree, and nature, of the radiative forcing.

Our analysis indicates that apparent AMO-like oscillatory variability during the past millennium is driven exclusively by volcanic radiative forcing because (i) spectral peaks are evident in the CMIP5 forced Last Millennium simulations but not in the control simulations; (ii) there is a common 50- to 70-year spectral peak in the LFV spectra of the individual ensemble members and the power spectrum of the ensemble average global average temperature series and EBM simulations (which reflect radiatively forced changes alone); and (iii) the associated signal exhibits a spatiotemporal pattern consistent with the response to tropical volcanic forcing, with peak tropical cooling synchronized with major volcanic-forcing episodes.

Other past studies have argued for a weaker and more limited role for radiative forcing (*43*, *44*). Knudsen *et al.* (*44*) assert that radiative forcing plays a dominant role only after 1800 CE and an "ambiguous" role before (1400 to 1800 CE). Wang *et al.* (*43*) claim a more consistent but still minor role, attributing only 30% of the AMO variance to the combined impact of solar and volcanic forcing and arguing for a multidecadal internal oscillation after the estimated forced component is removed. Both these studies, however, use a lagged correlation and regression analysis in an attempt to estimate and remove the forced signal, interpreting the residual series as an internal AMO oscillation. Attempts to remove estimates of forced variability from a time series containing both forced and unforced components, however, require a direct estimate of the forced component of response rather than simply the time series of the forcings alone, because a simple regression approach using raw forcing series cannot account for the temporal structure in the response to forcing (e.g., the decadal–time scale exponential recovery following impulsive volcanic forcing). That can be obtained using an EBM driven by estimated radiative forcings (*16*) or by averaging across an ensemble of forced coupled model simulations (*16*, *25*–*27*). We infer that these previous studies did not

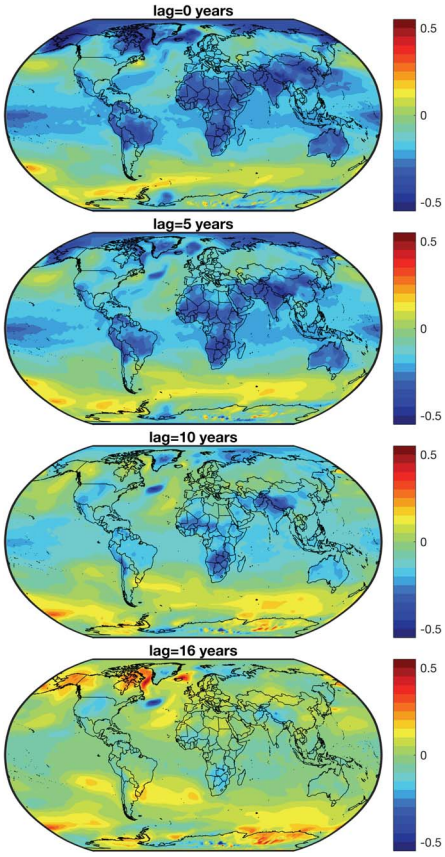

Fig. 4. Spatiotemporal evolution of multidecadal "signal" (centered at *f* = 0.016 cycle per year, ~63-year period) for CMIP5 GISS E2-R Last Millennium simulation. Shown is the progression of the signal during the first quarter cycle of evolution, depicting phase = 0 (lag = 0 years), 30° (lag = 5 years), 60° (lag = 10 years), and 90° (lag = 16 years), where the zero reference phase corresponds to peak tropical cooling. Color scale indicates temperature anomaly (°C).

fully account for, or remove, the forced signal before estimating the internal variability component.

The discrepancy with the Singh *et al.* (*40*) data-assimilation experiments is more perplexing. Although they find no evidence of narrowband multidecadal oscillatory behavior, our analysis of the same [Max Planck Institute (MPI)] simulation that they use in one of their two experiments shows a highly significant ($p < 0.01$) spectral peak (Fig. 2B and supplementary materials). There are at least two potential explanations for the discrepancy. First, as remarked earlier, their null result could simply be a consequence of a bias between the atmospheric states sampled by the real-world proxy data and the atmospheric states generated by the two models used, which would limit the fidelity of the resulting reconstruction in both the temporal and frequency domain. With data-assimilation experiments, it is difficult to determine if the source of a discrepancy can be attributed to the models used, the proxy data assimilated, or some combination of the two.

Second, Singh *et al.* (*40*) perform a spectral analysis of an AMO index defined as the average sea-surface temperature over the entire North Atlantic. Our multivariate (MTM-SVD) approach, by contrast, is based on an analysis of the entire field and the estimated spatial pattern of the signal. Substantial variation is displayed (Fig. 4) not just in the amplitude but also in the sign of associated temperature anomalies across the North Atlantic, implying some signal cancellation when averaging over the full North Atlantic domain. An index based on a simple average over the North Atlantic, consequently, tends to average away the signal and lower the effective signal-to-noise ratio, potentially rendering a true signal undetectable.

An additional feature of interest in the signal pattern (Fig. 4) is the apparent role of ocean dynamics in the delayed North Atlantic response to forcing, as noted earlier, which hints at features recognized in the limited modeling studies that have identified an internal AMO-oscillatory signal (*48*, *49*). For example, though focusing on solar rather than volcanic forcing, Waple *et al.* (*59*) speculate about the possibility that natural radiative forcing might resonate with internal modes of Atlantic multidecadal ocean-atmosphere variability.

The collective available evidence from instrumental and proxy observations and control and forced historical and Last Millennium climate model simulations points toward the existence of externally forced multidecadal oscillations that are a consequence of competing anthropogenic forcings during the historical era and the coincidental multidecadal pacing of explosive tropical volcanic activity in past centuries. There is no compelling evidence for a purely internal multidecadal AMO-like cycle.

A comprehensive analysis of the expanded paleoclimate proxy data now available should allow for further testing and refinement of these hypotheses, as should a detailed analysis of next-generation (CMIP6) control and forced last millennium multimodel ensembles, which may better capture ocean-atmosphere dynamics relevant to multidecadal climate variability.

REFERENCES AND NOTES

1. S. Power, T. Casey, C. Folland, A. Colman, V. Mehta, *Clim. Dyn.* **15**, 319–324 (1999).
2. B. Kirtman *et al.*, in *Climate Change 2013: The Physical Science Basis. Contribution of Working Group I to the Fifth Assessment Report of the Intergovernmental Panel on Climate Change*, T. F. Stocker *et al.*, Eds. (Cambridge Univ. Press, 2013).
3. G. A. Meehl, H. Teng, J. M. Arblaster, *Nat. Clim. Chang.* **4**, 898–902 (2014).
4. G. A. Meehl *et al.*, *Bull. Am. Meteorol. Soc.* **95**, 243–267 (2014).
5. N. J. Mantua, S. R. Hare, Y. Zhang, J. M. Wallace, R. C. Francis, *Bull. Am. Meteorol. Soc.* **78**, 1069–1079 (1997).
6. B. Henley, *Global Planet. Change* **155**, 42–55 (2017).
7. M. Newman *et al.*, *J. Clim.* **29**, 4399–4427 (2016).
8. M. E. Mann, J. Park, *J. Geophys. Res.* **99**, 25819 (1994).
9. M. E. Mann, J. Park, *J. Clim.* **9**, 2137–2162 (1996).
10. M. E. Mann, J. Park, *Adv. Geophys.* **41**, 1–131 (1999).
11. M. Latif, T. P. Barnett, *Science* **266**, 634–637 (1994).
12. C. K. Folland, D. E. Parker, F. E. Kates, *Nature* **310**, 670–673 (1984).
13. C. K. Folland, T. N. Palmer, D. E. Parker, *Nature* **320**, 602–607 (1986).
14. Y. M. Tourre, B. Rajagopalan, Y. Kushnir, *J. Clim.* **12**, 2285–2299 (1999).
15. M. E. Schlesinger, N. Ramankutty, *Nature* **367**, 723–726 (1994).
16. M. E. Mann, B. A. Steinman, S. K. Miller, *Geophys. Res. Lett.* **41**, 3211–3219 (2014).
17. A. Clement *et al.*, *Science* **350**, 320–324 (2015).
18. A. Clement *et al.*, *Science* **352**, 1527–1527 (2016).
19. M. A. Cane, A. C. Clement, L. N. Murphy, K. Bellomo, *J. Clim.* **30**, 7529–7553 (2017).
20. B. B. Booth, N. J. Dunstone, P. R. Halloran, T. Andrews, N. Bellouin, *Nature* **484**, 228–232 (2012).
21. A. Bellucci, A. Mariotti, S. Gualdi, *J. Clim.* **30**, 7317–7337 (2017).
22. L. N. Murphy, K. Bellomo, M. Cane, A. Clement, *Geophys. Res. Lett.* **44**, 2472–2480 (2017).
23. K. Bellomo, L. N. Murphy, M. A. Cane, A. C. Clement, L. M. Polvani, *Clim. Dyn.* **50**, 3687–3698 (2018).
24. K. Haustein *et al.*, *J. Clim.* **32**, 4893–4917 (2019).
25. M. E. Mann, K. A. Emanuel, *Eos* **87**, 233–241 (2006).
26. L. M. Frankcombe, M. H. England, M. E. Mann, B. A. Steinman, *J. Clim.* **28**, 8184–8202 (2015).
27. L. M. Frankcombe, M. H. England, J. Kajtar, M. E. Mann, B. A. Steinman, *J. Clim.* **31**, 5681–5693 (2018).
28. R. A. Kerr, *Science* **288**, 1984–1985 (2000).
29. K. E. Trenberth, D. J. Shea, *Geophys. Res. Lett.* **33**, L12704 (2006).
30. M. Ting, Y. Kushnir, R. Seager, C. Li, *J. Clim.* **22**, 1469–1481 (2009).
31. J. R. Knight, *J. Clim.* **22**, 1610–1625 (2009).
32. S. Wu, Z. Liu, R. Zhang, T. L. Delworth, *J. Oceanogr.* **67**, 27–35 (2011).
33. T. DelSole, M. K. Tippett, J. Shukla, *J. Clim.* **24**, 909–926 (2011).
34. D. Zanchettin, O. Bothe, W. Müller, J. Bader, J. H. Jungclaus, *Clim. Dyn.* **42**, 381–399 (2014).
35. R. Zhang, *Geophys. Res. Lett.* **44**, 7865–7875 (2017).
36. M. E. Mann, J. Park, R. S. Bradley, *Nature* **378**, 266–270 (1995).
37. T. F. Stocker, L. A. Mysak, *Clim. Change* **20**, 227–250 (1992).
38. R. D. D'Arrigo, E. R. Cook, M. E. Mann, G. C. Jacoby, *Geophys. Res. Lett.* **30**, 1549 (2003).
39. E. R. Cook, R. D. D'Arrigo, M. E. Mann, *J. Clim.* **15**, 1754–1765 (2002).
40. H. K. A. Singh, G. J. Hakim, R. Tardif, J. Emile-Geay, D. C. Noone, *Clim. Past* **14**, 157–174 (2018).
41. H. Fischer, B. A. Mieding, *Clim. Dyn.* **25**, 65–74 (2005).
42. S. T. Gray, L. J. Graumlich, J. L. Betancourt, G. T. Pederson, *Geophys. Res. Lett.* **31**, L12205 (2004).
43. J. Wang *et al.*, *Nat. Geosci.* **10**, 512–517 (2017).
44. M. F. Knudsen, B. H. Jacobsen, M.-S. Seidenkrantz, J. Olsen, *Nat. Commun.* **5**, 3323 (2014).
45. M. E. Mann *et al.*, *Science* **326**, 1256–1260 (2009).
46. H. Goosse *et al.*, *J. Geophys. Res.* **115**, D09108 (2010).
47. H. Goosse *et al.*, *Clim. Dyn.* **39**, 2847–2866 (2012).
48. T. L. Delworth, M. E. Mann, *Clim. Dyn.* **16**, 661–676 (2000).
49. J. R. Knight, R. J. Allan, C. K. Folland, M. Vellinga, M. E. Mann, *Geophys. Res. Lett.* **32**, L20708 (2005).
50. M. E. Mann, B. A. Steinman, S. K. Miller, *Nat. Commun.* **11**, 49 (2020).
51. Intergovernmental Panel on Climate Change, in *Climate Change 2013: The Physical Science Basis.* T.F. Stocker *et al.*, Eds. (Cambridge Univ. Press, 2013).
52. M. E. Mann, J. Lees, *Clim. Change* **33**, 409–445 (1996).
53. C. M. Ammann, P. Naveau, *Geophys. Res. Lett.* **30**, 1210 (2003).
54. B. A. Steinman, M. E. Mann, S. K. Miller, *Science* **347**, 988–991 (2015).
55. D. T. Shindell, G. A. Schmidt, M. E. Mann, G. Faluvegi, *J. Geophys. Res.* **109**, D05104 (2004).
56. Specifically, as in (*55*), we observe the highest-amplitude cooling responses over the tropical and subtropical continents. In addition, however, there is warming over mid-latitude regions of North America and Eurasia and cooling in polar and subpolar regions of North America and Siberia. Using model simulations with GISS ModelE, the authors show that these latter features are dynamically induced, associated with a positive AO-NAO–like cold-season atmospheric circulation response to tropical volcanic radiative forcing (see supplementary materials for a direct comparison).

57. J. Yang, C. Xiao, *Int. J. Climatol.* **38**, 1706–1717 (2018).
58. G. Müller-Plath, *Front. Earth Sci.* **8**, 559337 (2020).
59. A. Waple, M. E. Mann, R. S. Bradley, *Clim. Dyn.* **18**, 563–578 (2002).
60. M. E. Mann, *Geophys. Res. Lett.* **35**, L16708 (2004).

ACKNOWLEDGMENTS

We acknowledge the World Climate Research Programme's Working Group on Coupled Modelling, which is responsible for CMIP, and we thank the climate modeling groups for producing and making available their model output. **Funding:** M.E.M., B.A.S., D.J.B., and S.K.M. were supported by grants 1748097 and 1748115 from the NSF Paleoclimate Program. **Author contributions:** M.E.M. conceived, designed, and performed the research and wrote the paper. B.A.S., D.J.B., and S.K.M. performed some aspects of the research and co-wrote the paper. **Competing interests:** The authors declare no competing financial interests. **Data and materials availability:** All raw data and results from our analysis, as well as all Matlab code, are available at http://www.meteo.psu.edu/~mann/supplements/Mann_MTMSVD_2020.

SUPPLEMENTARY MATERIALS

science.sciencemag.org/content/371/6533/1014/suppl/DC1
Materials and Methods
Supplementary Text
Figs. S1 to S10
Tables S1 to S3
References (*61*–*97*)

1 May 2020; accepted 25 January 2021
10.1126/science.abc5810